Shahid Beheshti University

Sustainable Earth Trends

Journal homepage: http://sustainearth.sbu.ac.ir

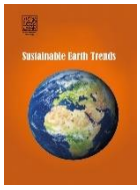

Spatio-temporal analysis of wind erosion hazard in Alborz and Qazvin provinces

Kimia Javaheri[a], Tayebeh Mesbahzadeh [a*], Hassan Khosravi[a], Hadi Eskandari Damaneh[b]

[a] Department of Arid and Mountainous Regions Reclamation, Faculty of Natural Resources, University of Tehran, Karaj, Iran
[b] Researcher of Desert Research Division, Research Institute of Forests and Rangelands, Agricultural Research Education and Extension Organization (AREEO), Tehran, Iran

ABSTRACT

In recent decades, human activities have intensified wind erosion, affecting 30% of the Earth's surface. This study evaluates land susceptibility to wind erosion and identifies dust sources in Alborz and Qazvin provinces using the ILSWE index, which integrates climatic erosivity, soil erodibility, soil crust factor, vegetation cover, and surface roughness. These factors were derived from climatic data, field observations, and laboratory analyses. Land use analysis (2001–2022) revealed a 3.82% decline in rangeland, while cropland (2.93%), barren land (3.01%), and urban areas (0.47%) increased. Savannas (0.12%) and shrublands (2.48%) decreased, while water bodies remained unchanged. The highest climatic erosivity was found in the northern, eastern, and southwestern regions. Vegetation cover and surface roughness peaked in the central to eastern areas, while the lowest values were observed in the northern, southern, and western regions. Soil crust and erodibility were highest in the southern, western, and southwestern areas, while the lowest values occurred in the central and northern parts. Over 70% of the region exhibited "very high" or "high" wind erosion sensitivity, with peaks in 2003, 2004, 2021, and 2022. Highly sensitive areas in the central and northwestern parts have decreased over time. Trend analysis showed that 8.45% of the region had reduced sensitivity (mainly in croplands), 81.82% remained stable, and 9.73% increased (mainly in barren lands and dust hotspots). The study concludes that climatic conditions, vegetation cover, and soil type contribute to wind erosion, while increasing barren and croplands reflect population growth and higher food demand.

ARTICLE INFO

Keywords:
Dust source
Trend of changes
Land use
ILSWE index

Article history:
Received: 10 March 2025
Accepted: 05 May 2025

*Corresponding author
E-mail address:
tmesbah@ut.ac.ir
(T. Mesbahzadeh)

Citation:
Javaheri, K. et al., (2026). Spatio-temporal analysis of wind erosion hazard in Alborz and Qazvin provinces, *Sustainable Earth Trends:* 6(1), (86-98).

DOI: 10.48308/set.2025.239124.1113

1. Introduction

Soil erosion has become one of the most serious natural hazards globally in the 21st century, posing significant challenges to the environment, agricultural productivity, and food security (Kestel et al., 2023). Wind erosion is a severe environmental threat leading to significant soil degradation in arid, semi-arid, and agricultural areas (Borrelli et al., 2015). This phenomenon is a complex geomorphic process influenced by various variables (Shao, 2008). Wind-driven soil particle movement occurs at the soil surface when three environmental conditions simultaneously exist: 1) Wind is strong enough to mobilize soil particles, 2) Soil characteristics make it susceptible to wind erosion (e.g., soil structure, organic matter content, and moisture), and 3) The surface is largely devoid of vegetation, rocks, or snow (Bagnold, 1941; Nordstrom and Hotta, 2004; Shao, 2008). Human activities and biogeochemical, biophysical, and hydrological factors frequently exacerbate soil erosion. Soil erosion rates and sensitivity maps provide information about vulnerable areas. However, evaluating soil erosion is highly complex due to its multifaceted impacts, which justify the diversity of mathematical models used to measure it (Selmy et al., 2021). Research has shown that emitted dust contains valuable fine soil components such as silt, clay, and organic

carbon (Sterk et al., 1996; Funk et al., 2008; Ravi et al., 2011). Studies have also indicated an increasing trend in wind erosion at various levels. Alipour et al. (2018) analyzed dust events in Qazvin and Alborz provinces and their relationship with drought during 2000-2014. Results showed that Qazvin and Karaj stations had the highest number of dusty days, with May and June being the peak months. No significant correlation was found between drought and dusty days in Karaj, but a weak correlation was observed in Qazvin.

Rangzan and Balouei (2024) examined the relationship between dust events and topographic factors, vegetation cover, and precipitation in Khuzestan province. Results indicated that elevation and slope direction had the highest correlation with dust reduction and increase, respectively. Statistical analyses also confirmed significant relationships between dust events and the investigated factors.

Their research emphasized the importance of remote sensing for identifying dust sources and combating desertification. Understanding the spatio-temporal patterns of land sensitivity to wind erosion is crucial for designing effective management strategies to control soil erosion. Soil erosion modeling becomes critical in developing and implementing soil management and conservation policies. A better understanding of the geographical distribution of soil erosion necessitates spatial models of soil erosion. Today, advancements in remote sensing and Geographic Information Systems (GIS) provide up-to-date, high-quality data for researchers to analyze wind erosion trends and enhance modeling accuracy. Geoinformatics technologies, such as GIS and remote sensing, assist in obtaining various data types, which are then integrated with different soil erosion models for evaluation (Selmy et al., 2021; Salajegheh et al., 2024).

The Index of Land Susceptibility to Wind Erosion (ILSWE), proposed by Borrelli et al. (2016), is a reliable model for assessing wind erosion. This model relies on various factors, including climatic erosivity, soil erodibility, soil crust factor, vegetation cover, and surface roughness, derived from comprehensive climatic data measurements, field observations, and laboratory analyses. Climate data and field surveys, combined with remote sensing imagery, were used to develop five qualitative indices (soil, climate, vegetation, land management, and wind erosion indices). Borrelli et al. (2016) conducted a study presenting a preliminary pan-European assessment of land susceptibility to wind erosion using the ILSWE model. The sensitivity of each factor was ranked using fuzzy logic. The results indicated that this approach is suitable for integrating wind erosion data with environmental variables. In 34 European countries, between 2.9% and 5.3% of the total land area was predicted to have moderate to high susceptibility to wind erosion. These findings provided a solid foundation for future research on the spatial variability of land susceptibility to wind erosion across Europe.

Selmy et al. (2021) found that designing spatial models of soil erosion using existing data sources and integrating the Universal Soil Loss Equation (USLE) and ILSWE with GIS techniques is suitable for calculating soil erosion.

Fadl et al. (2021) combined the ILSWE with the Modified Mediterranean Desertification and Land Use (MEDALUS) method to create a GIS-based model for desertification intensity mapping. Their results showed that the proposed model was an effective tool for monitoring vulnerable areas.

Kestel et al. (2023) used the ILSWE index to analyze the spatio-temporal variability of wind erosion hazard in South Africa between 2005 and 2019.

The study identified wind erosion-prone areas and annual periods for further analysis and conservation policies aimed at prioritizing mitigation and adaptation strategies. Based on the literature review, this study aims to model wind erosion using the ILSWE remote sensing climatic model and examine wind erosion trends in Alborz and Qazvin provinces from 2001 to 2022. Dust storms, as one of the major environmental challenges, persistently affect Alborz Province and other regions worldwide. This phenomenon seriously impacts human health, regional air quality, and the environment. Analyzing dust storms and identifying the contributing factors in Alborz Province is crucial, especially considering that a significant portion of dust sources originates within the region. One of the limitations of this study is the lack of access to data at finer spatial scales, which would have allowed for a more detailed analysis.

2. Material and methods

2.1. Study area

The provinces of Alborz and Qazvin, located in northern Iran, are considered as a single study unit in this research (Fig. 1). Alborz province is situated between 35°32′ to 36°20′ N latitude and 50°09′ to 51°27′ E longitude, while Qazvin province is located between 48°45′ to 50°50′ E longitude and 35°37′ to 36°45′ N latitude. In this study area, the minimum elevation is 235 meters, and the maximum reaches 4,101 meters. This region is bordered by Mazandaran and Gilan provinces to the north, Markazi and Hamedan provinces to the south, Tehran province to the east, and Zanjan province to the west (Mesbahzadeh et al., 2018). In Alborz, rainfall starts in November and December and continues until mid-May. The southern areas have a desert climate, while the northern regions experience semi-humid to humid climates. Vegetation cover grows adequately only in spring and in years with high precipitation. Due to excessive livestock grazing, the rangelands have lost their productivity, leading to an increased risk of soil erosion (Zahrabi et al., 2020). Qazvin province also has three climatic zones: semi-arid, semi-humid, and humid, with the majority of the area falling within the semi-arid zone (Zandifar et al., 2022; Eskandari Damaneh, et al., 2022).

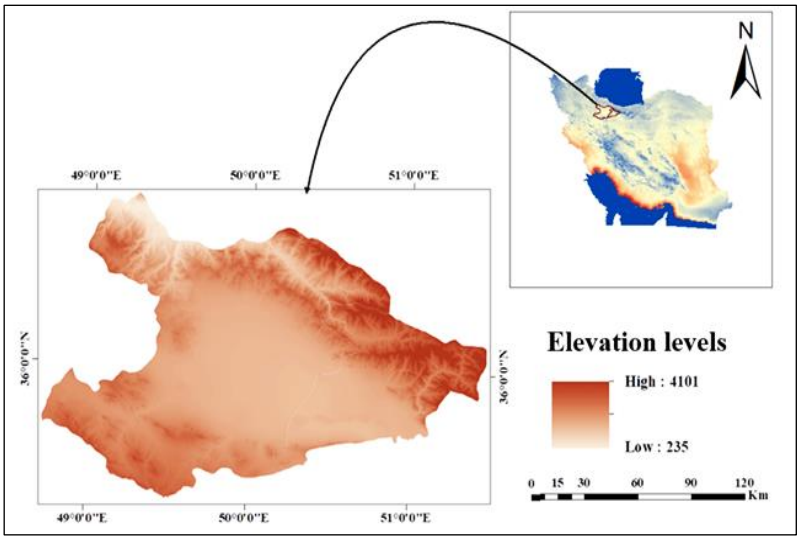

Fig. 1. Geographic location of the study area (Alborz and Qazvin).

2.2. Dataset

To analyze the dust phenomenon in the study area, the required meteorological data—including wind speed and direction, temperature, precipitation, and minimum horizontal visibility—were obtained from the website of the Iran Meteorological Organization (https://data.irimo.ir/) for synoptic stations in Alborz and Qazvin provinces. Data on potential evapotranspiration (PET) and precipitation (Pre) were retrieved from https://data.ceda.ac.uk. This platform is an online data repository that facilitates the sharing and access to datasets related to earth sciences, environmental studies, climatology, and related fields. It is managed by the Centre for Environmental Data Analysis (CEDA) in the United Kingdom. Additionally, wind speed (WS) data were obtained from the climatology data portal at www.climatologylab.org. Soil texture maps, including sand, silt, clay, and organic matter content, were extracted from the SoilGrids database (https://soilgrids.org/), which provides information on various soil parameters at different depths for any given geographic coordinate. Calcium carbonate ($CaCO_3$) content data were acquired from the FAO's Harmonized World Soil Database (HWSD) (https://www.fao.org/soils-portal/data-hub/soil-maps-and databases/harmonized-world-soil-database-v20/en/).

Vegetation cover was represented using vegetation indices derived from satellite imagery. Specifically, this study utilized the 1-km resolution MODIS MOD13A3 monthly vegetation index products. Normalized Difference Vegetation Index (NDVI) maps were acquired from the EarthData database (https://appeears.earthdatacloud.nasa.gov/).

To assess surface roughness, MODIS land cover product (MCD12Q1.061) imagery was

employed. After preparation, all final maps for the relevant factors were resampled to a spatial resolution of 250 meters.

2.3. Methodology

In this study, remote sensing data were used to assess land sensitivity to wind erosion. The required data were obtained from databases and then utilized to develop a land sensitivity model for wind erosion.

2.3.1. Index of land susceptibility to wind erosion (ILSWE)

Wind erosion is a complex process influenced by multiple factors, making it challenging to define comprehensive criteria for evaluating these factors at regional scales. Therefore, wind erosion studies at the regional scale use complexity reduction strategies while maintaining the main factors influencing wind erosion (Selmy et al., 2021). Consequently, Fenta et al. (2020) developed the Index of Land Susceptibility to Wind Erosion (ILSWE), which is used in this study to estimate and assess the intensity and risks of soil erosion by integrating layers describing the key factors, including Climatic Erosivity (CE), Soil Erodibility (EF), Soil Crust (SC), Vegetation Cover (VC), and Surface Roughness (SR). This index is calculated using Eq. 1 as follows.

$$\mathrm{ILSWE} = \mathrm{f}(\mathrm{CE} \times \mathrm{EF} \times \mathrm{SC} \times \mathrm{VC} \times \mathrm{SR}) \quad (1)$$

Here, CE represents Climatic Erosivity, EF stands for Soil Erodibility, SC denotes Soil Crust, VC is Vegetation Cover, and SR refers to Surface Roughness.

2.3.1.1. Climatic erosivity factor

The CE factor determines the average rate of movement of surface soil particles in relation to the amount of moisture and the average wind speed (Skidmore, 1986). In this study, a proposed model by Chepil et al. (1962), as revised by FAO (1979), is used. This factor aligns most closely with arid regions, as the CE factor, when rainfall reaches zero, is solely dependent on wind speed. However, when rainfall equals potential evapotranspiration, the CE value becomes zero (Skidmore, 1986). The climatic erosivity factor is calculated using Eq. 2.

$$\mathrm{CE} = \frac{1}{100} \times \sum_{\mathrm{i}=1}^{\mathrm{i}=12} \mathrm{u_i^3} \times \frac{(\mathrm{PET_i} - \mathrm{P_i})}{\mathrm{PET_i}} \times \mathrm{d_i} \quad (2)$$

In this equation, u_i is the monthly mean wind speed (m/s) for month i, PET_i is the potential evapotranspiration for month i, P_i is the precipitation for month i, and d_i is the number of days in month ii.

2.3.1.2. Soil erodibility factor

The EF factor describes the susceptibility of the bare soil surface to the shear force generated by wind due to the specific characteristics of the soil (Colazo and Buschiazzo, 2010). The EF factor of soil is determined by the proportion of erodible soil aggregates, along with organic carbon content and clay, which are the main factors that enhance the stability of aggregates by binding soil particles together (Fryrear, 1980; Skidmore and Layton, 1992). The calculation of the EF factor involves the basic physical and chemical properties of the soil. Eq. 3 corresponds to the soil erodibility factor.

$$\mathrm{EF} = \frac{29 \cdot 09 + (0 \cdot 31 \times \mathrm{SA}) + (0 \cdot 17 \times \mathrm{SI}) + \left(0 \cdot 33 \times \frac{\mathrm{SA}}{\mathrm{CL}}\right) - (2 \cdot 59 \times \mathrm{OM}) - (0 \cdot 95 \times \mathrm{CaCO3})}{100} \quad (3)$$

In this equation, $SA =$ sand percentage, $SI =$ silt percentage, $CL =$ clay percentage, and $OM =$ organic matter percentage of the soil.

2.3.1.3. Soil crust factor

Most studies, considering the reducing effect of soil crusts on wind erosion (Belnap, 2003; Eldridge and Leys, 2003; Zhang et al., 2006), have included the soil crust factor (SCSC) in the ILSWE. This factor is applied based on a regressive erosion coefficient related to the amount of clay and organic matter (Fryrear et al., 1998). Eq. 4 corresponds to the soil erodibility factor.

$$\mathrm{C} = \frac{1}{1 + (0 \cdot 006 \times \mathrm{CL}^2) + (0 \cdot 21 \times \mathrm{MO}^2)} \quad (4)$$

In this equation, CL is the percentage of clay, and OM is the percentage of soil organic matter.

2.3.1.4. Vegetation cover factor

The vegetation cover factor (VC) was obtained using vegetation cover data from MODIS 1 km resolution images (MOD13A3) on a monthly basis (Eskandari Damaneh et al., 2024). The calculation of VC was performed based on the NDVI values of very dense vegetation ($NDVI_V$) and bare soil ($NDVI_S$) using Eq. 5.

$$\mathrm{F_{cover}} = \frac{\mathrm{NDVI} - \mathrm{NDVI_S}}{\mathrm{NDVI_V} - \mathrm{NDVI_S}} \quad (5)$$

In this equation, $NDVI =$ annual mean map, $NDVI =$ index value for bare soil, and $NDVI_V =$ index value for dense vegetation (Selmy et al., 2021).

2.3.1.5. Surface roughness factor

Surface roughness refers to the natural and man-made vertical irregularities of the land, which reduce wind speed near the ground surface in an inverse logarithmic relationship (Fadl et al., 2021; Eskandari Damaneh et al., 2022). In this study, the standard provided by TA–LUFT (2001) will be used. Table 1 shows the average roughness length in different land use and land cover classes.

Table 1. Average roughness length in land use and land cover classes (TA-Luft, 2001).

Land Use and Land Cover	Z_0
Barren lands, sand dunes, seasonal wetlands	0.01
Poor natural rangelands, salt marshes	0.02
Mines, rainfed agricultural lands, and coastal wetlands	0.05
Green urban areas, vineyards, irrigated agricultural lands, medium to good rangelands, grasslands with scattered trees	0.2
Orchards, forest shrubs	0.5
Discontinuous urban areas, industrial or commercial complexes, coniferous forests (needle-leaved trees)	1
Broad-leaved forests and mixed forests	1.5
Continuous urban areas	2

2.3.2. Preparation of the ILSWE Map

After preparing the final maps for each factor, all the maps were resampled at a 250-meter scale. Then, based on the impact of each factor on wind erosion, the maps were classified into 5 categories: very low, low, moderate, high, and very high (Borrelli et al., 2016), using the Natural Breaks method and the Jenks and Caspal algorithm. This classification method aims to reduce variance within the classes while maximizing variance between the classes (Kestel et al., 2023). In the next step, the classified maps were normalized, and finally, by multiplying the 5 factors together, the final ILSWE index map for the years 2022-2001 was obtained.

2.3.2.1. Trend Analysis

The trend of changes in the ILSWI index during the period 2022-2001 for each pixel of the image was simulated using linear regression in the QGIS software, based on the following Eq. 6:

$$\theta_{slope} = \frac{n \times \sum_{j=1}^{n} j \times X_j - \sum_{j=1}^{n} j \times \sum_{j=1}^{n} X_i}{N \times \sum_{j=1}^{n} j^2 - \left[\sum_{j=1}^{n} j\right]^2} \quad (6)$$

In this equation, θ_{slope} represents the slope of the changes in the index of interest in the study area, n is the time period considered for monitoring, X_i is the value of the index for time period j, and $0 < \theta_{slope}$ and $0 > \theta_{slope}$ indicate positive and negative trends in the changes of the respective index, respectively (Eskandari Damaneh et al., 2021).

2.3.2.2. Analysis of Land Use Change Trends

To investigate land use changes in the study area during the period from 2022 to 2001, MODIS satellite images (MCD12Q1.061) were used (Shobeiri et al., 2025). After opening the land use layers in the ArcMap environment, the study area boundary was clipped using the Extract by Mask tool. Then, in the resulting layer, an "Editor" session was started, and a field called LULC (Land Use/Land Cover) was added in Text format to input the type of land use. Additionally, another field titled SR (Surface Reflection) in Text format was added for land use values based on the TA-LUFT table. In the final step, the obtained layers were analyzed annually and then calibrated with field data.

2.4. Land use map preparation

In this study, land use maps were obtained from the Earth Data website. To assess land use, MODIS satellite imagery (MCD12Q1.061) was used. After importing the land use layers into ArcMap, the boundary of the study area was clipped. Then, a field called LULC was added to the resulting layer to include the land use type, which was determined according to the TA–LUFT table.

Finally, to validate the obtained land uses, they were calibrated with field observation points. The workflow chart is shown in Fig. 2.

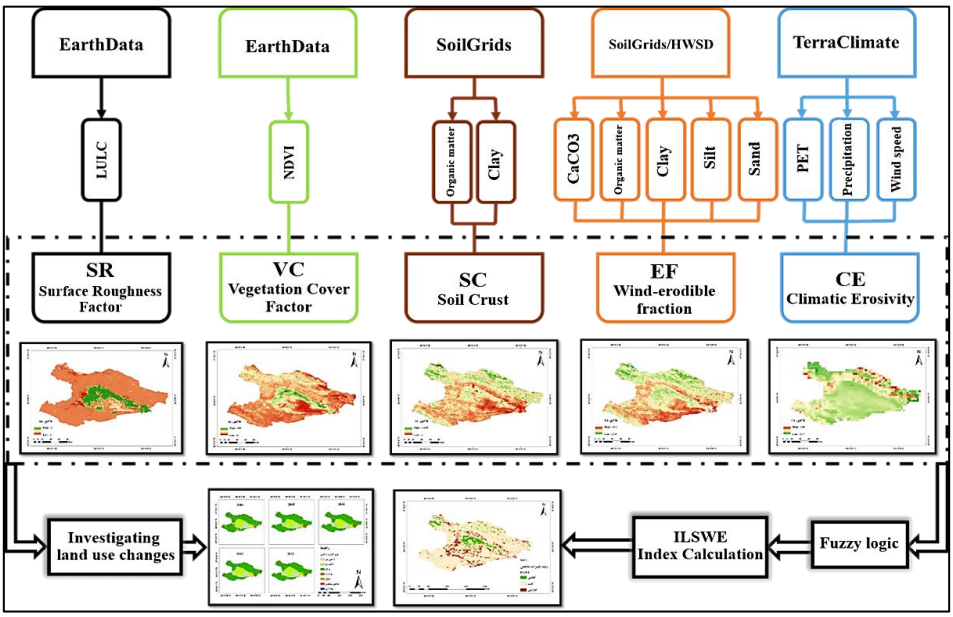

Fig. 2. Workflow chart of the methodology.

3. Results and discussion

3.1. Analysis of land use change in the study area for the period 2001-2022

The analysis of land use changes in the study area for the period 2001-2022 is shown in Figs 3 and 4. On average, seven types of land use were observed, including barren land, cropland, rangelands, shrubland, savannas, urban areas, and water bodies. Rangelands, followed by croplands occupied the largest area during 2001-2022. The percentage of the area for each land use type over the years 2001-2022 is presented in Table 2. According to the results, and as shown in Figs 3 and 4, the area of barren land increased from 11.97% to 14.98%, cropland increased from 18.03% to 20.96%, rangeland area decreased from 61.91% to 58.09%, shrubland area decreased from 5.83% to 3.35%, savanna area decreased from 0.23% to 0.11%, and urban area increased from 1.96% to 2.43%. The extent of water bodies remained stable at 0.1% over the 22-year period.

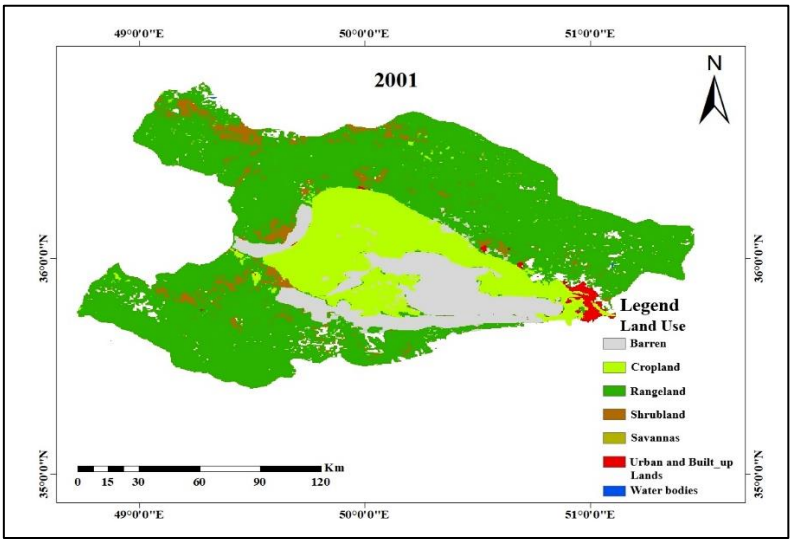

Fig. 3. Land use in the study area in the year 2001.

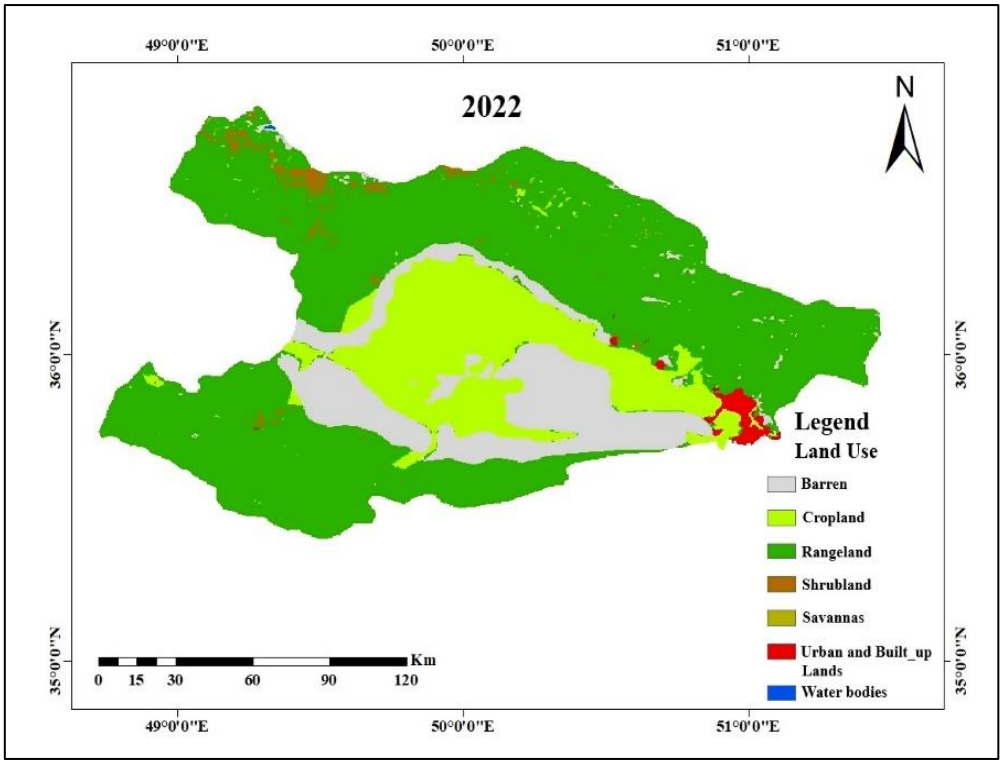

Fig. 4. Land use in the study area in the year 2022.

Table 2. The land use changes of the study area during the period 2001–2022.

Land use	Area (%) 2001	Area (%) 2022	Area changes (%) 2001-2022
Barren	11.97	14.98	3.01
Croplands	18.03	20.96	2.93
Rangelands	61.91	58.09	-3.82
Open Shrublands	5.83	3.35	-2.48
Savannas*	0.23	0.11	-0.12
Urban and Built-up Lands	1.96	2.43	0.47
Water Bodies	0.1	0.1	0.00
Sum	100	100	

*Savannas are tropical or subtropical ecosystems characterized by a mixture of grasses and scattered trees, typically found in regions with seasonal rainfall patterns (Scholes and Archer, 1997).

3.2. Investigation of changes in soil sensitivity factors to wind erosion in the 2022-2001 period

Figs 5a to 5e present the investigation of changes in the factors of climatic erosivity (CE), vegetation cover (VC), surface roughness (SR), soil erodibility (EF), and soil crust (SC) during the 2022-2001 period.

An analysis of the changes in the climatic factor CE (Fig. 5a) reveals that its average value is approximately 75.5. The spatial changes of this factor show that the maximum values are found in the northern, eastern, and, to some extent, southwestern regions, whereas the minimum values occur in the central, southern, and southeastern parts of the study area.

The changes in the vegetation cover (VC) and surface roughness (SR) factors (Figs 5b and 5c) show that the average values for VC and SR are approximately 43.5 and 2.4, respectively. The spatial distribution of these factors indicates that the maximum values are located in the central to eastern regions, while the minimum values are found in the northern, southern, and western areas of the study region.

Lastly, the analysis of the soil crust (SC) and soil erodibility (EF) factors (Fig 5d and 5e) reveals that the average values for SC and EF are 0.45 and 0.44, respectively. Spatially, the maximum values of these factors are found in the southern, western, and southwestern regions, while the minimum values are located in the central and northern parts of the study area.

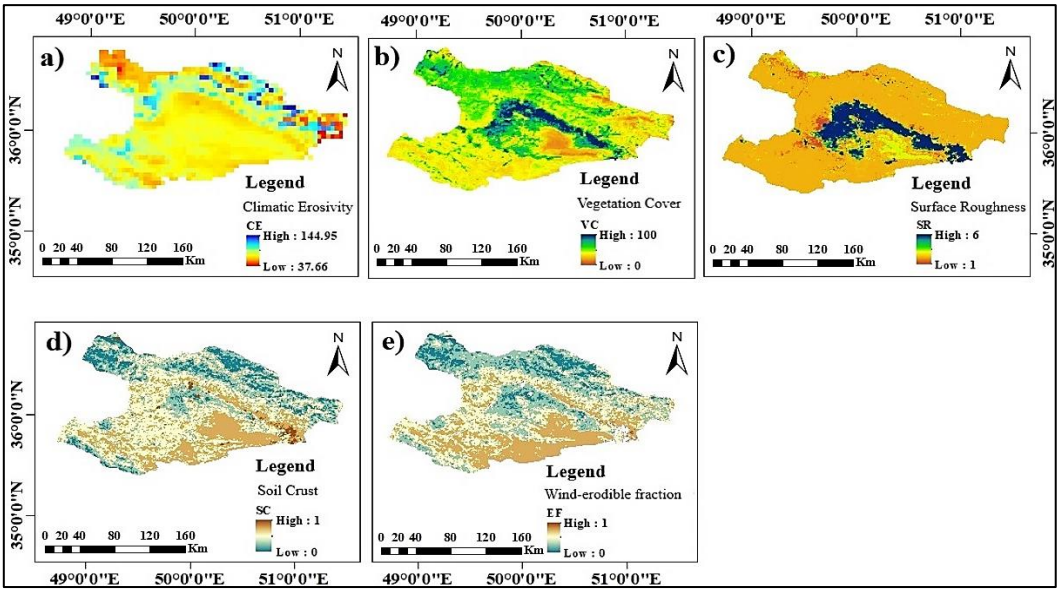

Fig. 5. Factors of a) Climatic Erosivity, b) Vegetation Cover, c) Surface Roughness, d) Soil Crust, e) Soil Erodibility, in the period from 2001 to 2022.

3.3. Analysis of temporal and spatial changes of the ILSWE index in the period 2001-2022

The analysis of temporal and spatial changes of the annual ILSWE index over the 22-year period from 2001 to 2022 is presented in Figs 6 and 7. The 22-year average map of the ILSWE index is also shown in Fig. 8. The examination of changes in the different classes of the ILSWE index shows that more than 70% of the region was categorized in the very high and high classes, with only in the years 2003, 2004, 2021, and 2022, where the percentages were 57.93%, 59.13%, 67.58%, and 68.46%, respectively. The spatial variation of the ILSWE index in Fig. 7 shows that, overall, areas sensitive to wind erosion in the central parts, from east to west, and in the northern and northwestern sections, have been decreasing, with the very high erosion class declining over the 22 years. The analysis of interannual changes of the ILSWE index in Fig. 9 shows that the trend of changes varied between years. However, it is evident that these changes predominantly occurred in the moderate, high, and very high classes. Specifically, between 2001 and 2002, there was a decrease in moderate and high classes, with an approximately 18% increase in the very high class. Between 2002 and 2003, there was a 49% decrease in the very high class, accompanied by an increase in all classes, especially the high class. Between 2004 and 2005, the exceptionally high class increased by about 49%, while all other classes, particularly the high and moderate classes, decreased. Between 2013 and 2014, there was a 34% decrease in the very high class, with an increase in all classes, especially the high class. Lastly, between 2021 and 2022, the very high class decreased by approximately 5%, with an increase in the high class. Based on the annual precipitation variation chart, these sudden changes in the ILSWE classes can be attributed to abrupt fluctuations in precipitation levels (Fig. 10).

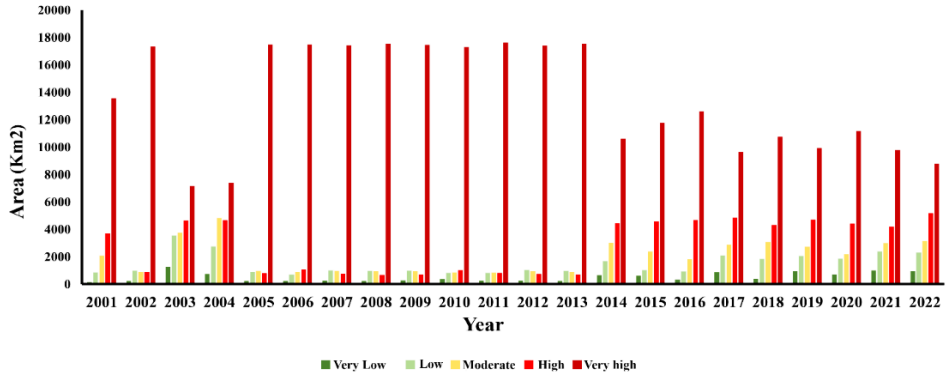

Fig. 6. Temporal changes of the annual ILSWE index over the 22-year period from 2001 to 2022.

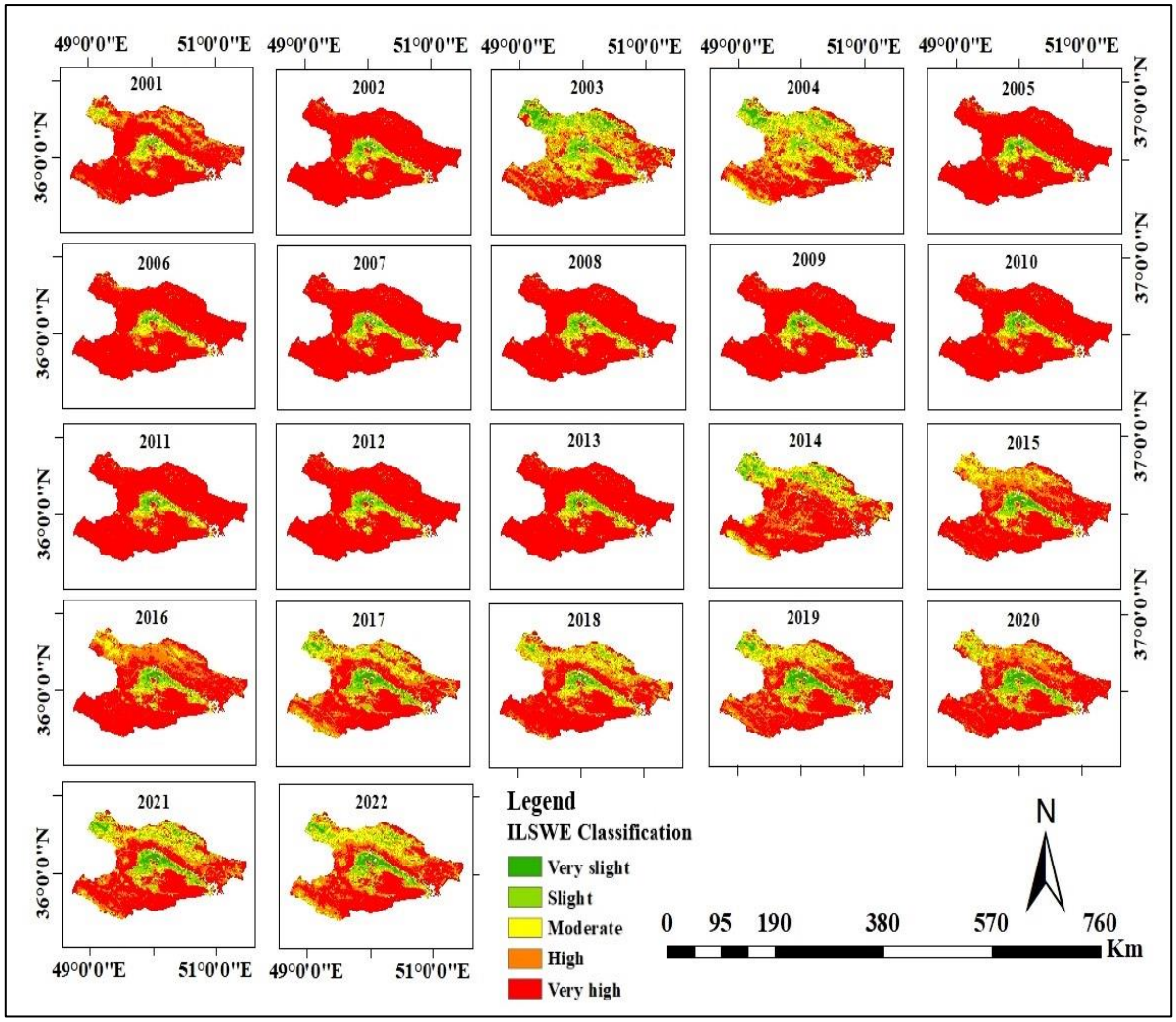

Fig. 7. Spatial changes of the annual ILSWE index over the 22-year period from 2001 to 2022.

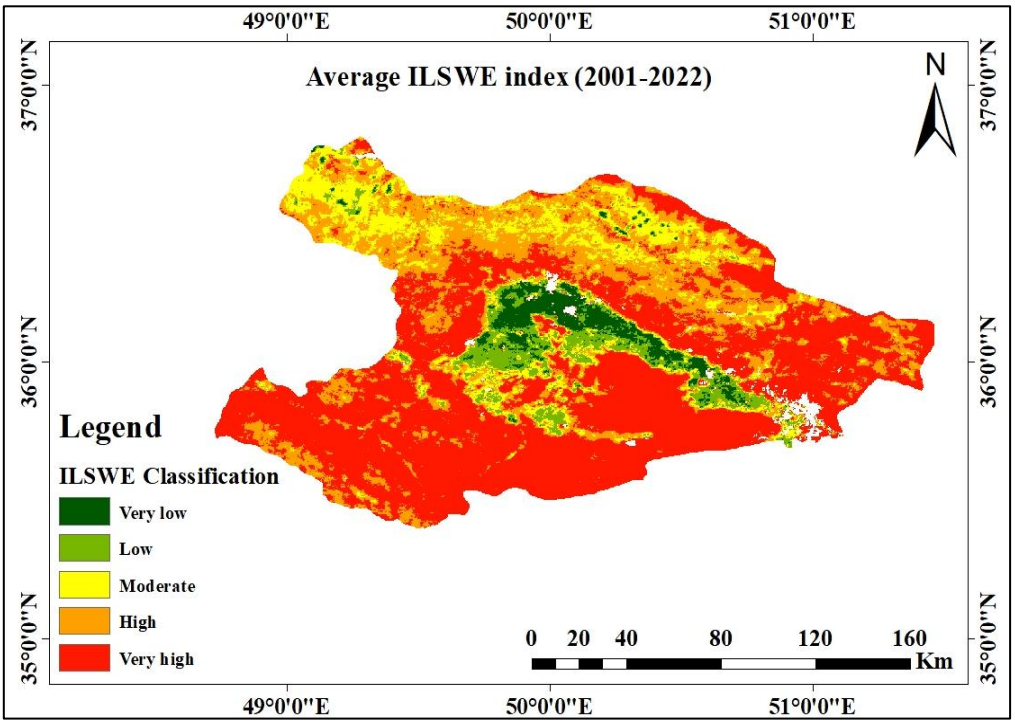

Fig. 8. Average ILSWE index (for the period 2001 to 2022).

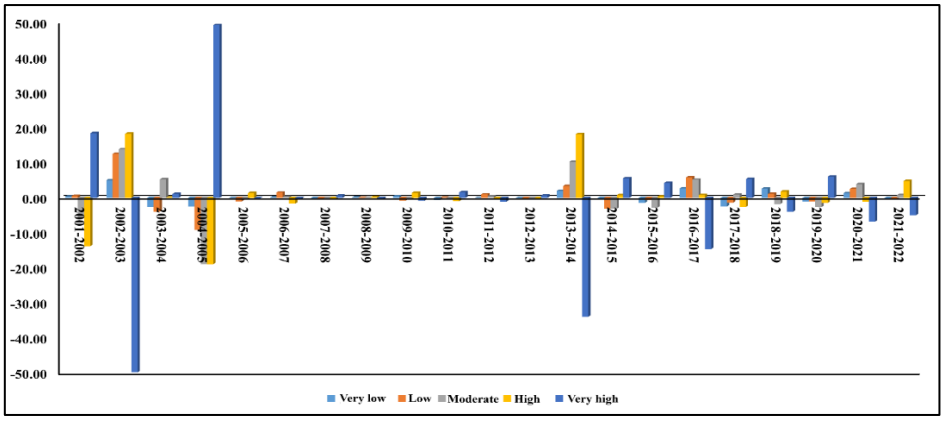

Fig. 9. Inter-annual changes of the ILSWE index.

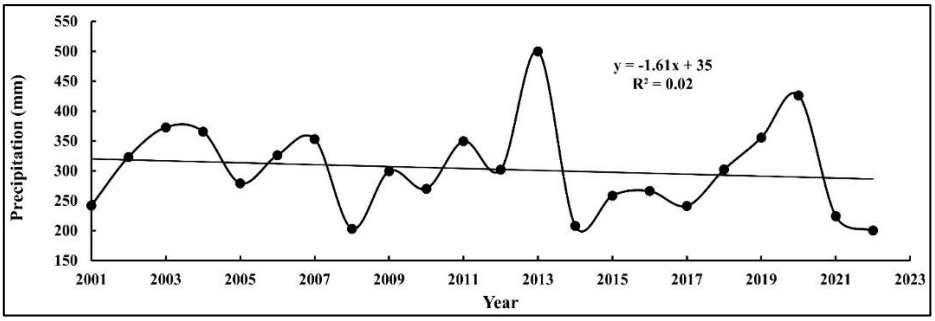

Fig. 10. The trend of annual average precipitation changes during the period from 2001 to 2022.

The analysis of the trend of ILSWE changes during the 2001-2022 period shows that approximately 8.45% of the study area exhibits a decreasing trend, 81.82% has a stable trend, and 9.73% of the area shows an increasing trend in sensitivity to wind erosion (Fig. 11). The majority of areas with a decreasing trend in wind erosion sensitivity are located from east to west across the study area, particularly in croplands. This is consistent with the increase in cropland during the 2001-2022 period. In these areas, the decreasing trend in sensitivity is influenced by the increase in very low to moderate classes of the ILSWE index. Scattered small areas with an increasing trend in wind erosion sensitivity are mainly found in locations where barren lands increased during the 2001-2022 period. These areas are identified as dust hotspots, where the very high class of the ILSWE index has had the greatest impact on the expansion of barren lands.

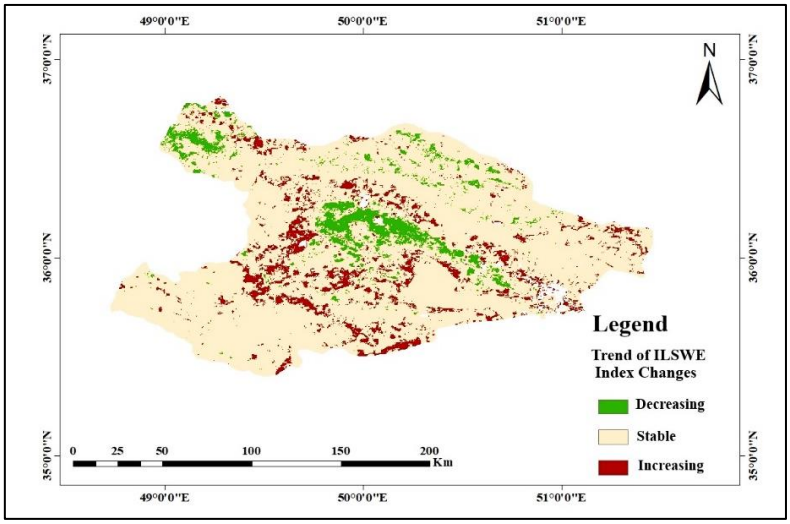

Fig. 11. Trend of ILSWE changes during the 2001-2022 period.

Wind erosion is a serious environmental hazard that leads to land degradation, air pollution, and negative impacts on human health (Singh, 2023). With the development of remote sensing (RS) techniques and geographic information systems (GIS), large-scale erosion models have become more flexible. They can be assessed quickly (Abuzaid et al., 2023). Therefore, to assess wind erosion in the provinces of Qazvin and Alborz, the ILSWE model was used based on remote sensing, climate, and soil data. The results indicate that, considering the climatic conditions, vegetation cover, and the type of soil in the studied region, this area is prone to wind erosion.

According to the conducted studies, seven types of land use were observed in the study area, including barren land, cropland, rangelands, shrublands, savannas, urban areas, and water bodies. Over the period 2022-2001, an increase of 3.01% in barren land, 2.93% in cropland, and 0.47% in urban areas was observed. Additionally, a decrease in the area of rangelands by 3.82%, shrublands by 2.48%, and savannas by 0.12% was observed during the same period. Throughout the 2001-2022 period, the area of water bodies remained unchanged.

Considering the population growth, the subsequent expansion of urban areas, and urbanization in the study area, barren land saw the most significant increase. Also, the largest increase in cropland was observed in the central part of the study area, which can be attributed to population growth and the increasing need for agriculture and food supply. In this regard, Kakavand et al. (2023) studied the optimization of water distribution methods in Qazvin province due to the growing population and the need for water for agriculture.

Due to recent climate changes, including reduced rainfall, increased temperature, and evaporation, available water for agriculture has decreased. On the other hand, the Salehieh Wetland is located in the southern part of the study area, which is drying up due to recent climatic changes and human activities. Given these factors, the available water for agriculture has significantly reduced, prompting farmers to use groundwater sources for irrigation (Eskandari Damaneh and Ghasemi Aryan, 2025). This, in turn, worsens the desertification of the region and increases the potential for wind erosion. In this context, Banihashemi Tarshizi et al. (2021) studies showed that drought events in Qazvin province are expected to become more severe in the future. The results of the studies by Pelous and Taati (2022) also showed an increasing trend in croplands in Qazvin Plain. Additionally, the findings of Bagherpour et al. (2023) revealed that in recent years, due to continuous droughts, reduced rainfall, low relative humidity, and improper exploitation of the environment, such as excessive use of water resources and the implementation of surface water collection projects and drainage construction, the Salehieh Wetland has dried up, resulting in decreased soil moisture and dust storms.

4. Conclusion

Dust storms are natural phenomena that occur particularly in arid and semi-arid regions. Alborz Province has been significantly affected by this phenomenon in recent years due to its specific climatic conditions. Dust storms can have numerous negative impacts on the environment and human health, including reduced air quality, decreased visibility, and an increase in respiratory diseases. With the advancement of remote sensing (RS) and geographic information system (GIS) technologies, large-scale erosion models have become more flexible and can be analyzed in a shorter time (Abuzaid et al., 2023). Therefore, to assess wind erosion in Qazvin and Alborz provinces, the ILSWE model was employed based on remote sensing data, climatic variables, and soil information. The results indicate that, considering the study area's climatic conditions, vegetation cover, and soil types, the region has a notable potential for wind erosion. The management of areas susceptible to wind erosion requires comprehensive and multi-dimensional approaches. These approaches include improving agricultural practices, such as the use of cover crops, maintaining soil moisture, and reducing tillage, to prevent soil degradation, as well as implementing vegetation restoration programs in arid and semi-arid regions to reduce dust generation. Limiting industrial and construction activities in erosion-prone areas during critical periods, enforcing regulations to reduce pollution, and controlling agricultural and industrial operations are also essential.

Furthermore, supporting scientific research on the factors contributing to dust generation and management strategies, continuously evaluating the effectiveness of implemented measures, and updating management strategies based on new findings should be prioritized. Implementing these measures requires coordinated efforts and collaboration among governmental institutions, local communities, and non-governmental organizations. It is also crucial that sectoral decision-makers incorporate dust-related research findings into their planning and policy-making processes.

Acknowledgments

This research was conducted as part of a thesis project. Special thanks are extended to the Department of Reclamation of Arid and Mountainous Regions, Faculty of Natural Resources, University of Tehran, for their valuable support.

References

Abuzaid, A., El-Shirbeny, M. & Fadl, M., 2023. A new attempt for modeling erosion risks using remote sensing-based mapping and the index of land susceptibility to wind erosion. *Catena*, 227.

Alipour, N., Mesbahzadeh, T., Ahmadi, H., Malkian, A. & Jafari, M., 2018. Synoptic Analysis of Dust Events and Their Relationship with Drought in Qazvin and Alborz Provinces. *Geography Quarterly (Regional Planning)*, 8(30), 59–68.

Bagherpour, M., Tabatabaie, F., Zare, S., Nazari Samani, A.A. & Ghoohestani, G., 2023. Evaluating the changes in the water body of Salehiyeh Wetland caused by the construction of drainage. *Journal of Arid Biome*, 13(2), 107-123.

Bagnold, R.A., 1941. *The Physics of Blown Sand and Desert Dunes*. Methuen and Company, London, 265p.

Banihashemi Tarshizi, S., Eslamian, S.S. & Nazari, B., 2021. Prediction of Local Alterations in the Relative Amounts of Temperature and Precipitation Caused by Climate Change in Near and Far Future, and Drought Investigation Using SPI and SPEI Indices in Qazvin Plain, Iran. *Journal of Water and Soil Science*, 25(2), 25-44.

Belnap, J., 2003. Biological soil crusts and wind erosion. In J. Belnap & O.L. Lange (Eds.), *Biological soil crusts: Structure, function, and management, ecological studies*. (pp. 339–347). Springer.

Borrelli, P., Panagos, P. & Montanarella, L., 2015. New insights into the geography and modelling of wind erosion in the European agricultural land. *Application of a spatially explicit indicator of land susceptibility to wind erosion. Sustainability*, 7(7), 8823-8836.

Borrelli, P., Panagos, P., Ballabio, C., Lugato, E., Weynants, M. & Montanarella, L., 2016. Towards a pan-European assessment of land susceptibility to wind erosion. *Land Degradation & Development*, 27(4), 1093-1105.

Chepil, W.S., Siddoway, F.H. & Armbrust, D.V., 1962. Climatic factor for estimating wind erodibility of farm fields. *Journal of Soil and Water Conservation*, 17, 162–165.

Colazo, J.C. & Buschiazzo, D.E., 2010. Soil dry aggregate stability and wind erodible fraction in a semiarid environment of Argentina. *Geoderma*, 159, 228–236.

Eldridge, D.J. & Leys, J.F., 2003. Exploring some relationships between biological soil crusts, soil aggregation and wind erosion. *Journal of Arid Environments*, 53, 457–466.

Eskandari Damaneh, H., Gholami, H., Mahdavi, R., Khoorani, A. & Li, J., 2021. Assessing the land degradation using water use efficiency (WUE) and drought indices (case study: Fars's province). *Journal of Range and Watershed Managment*, 74(1), 103-120.

Eskandari Damaneh, H., Gholami, H., Mahdavi, R., Khoorani, A. & Li, J., 2022. Evaluation of land degradation trend using satellite imagery and climatic data (Case study: Fars's province). *Desert Ecosystem Engineering*, 8(24), 49-64.

Eskandari Damaneh, H. & Ghasemi Aryan, Y., 2025. Investigating the trend and explaining the key drivers of desertification and land degradation in Salehiyeh wetland and Qazvin salt plain. *Integrated Watershed Management*, 4(4), 81-93.

Eskandari Damaneh, H., Khosravi, H. & Eskandari Damaneh, H., 2024. Investigating the land use changes effects on the surface temperature using Landsat satellite data. In *Remote Sensing of Soil and Land Surface Processes* (pp. 155-174). Elsevier.

Fadl, M.E., Abuzaid, A.S., AbdelRahman, M.A.E. & Biswas, A., 2021. Evaluation of Desertification Severity in El-Farafra Oasis, Western Desert of Egypt: Application of Modified MEDALUS Approach Using Wind Erosion Index and Factor Analysis. *Land*, 11, 54.

FAO., 1979. A provisional methodology for soil degradation assessment Food and Agriculture Organization of the United Nations.

Fenta, A.A., Tsunekawa, A., Haregeweyn, N., Poesen, J., Tsubo, M., Borrelli, P. & Kawai, T., 2020. Land susceptibility to water and wind erosion risks in the East Africa region. *Science of the Total Environment*, 703, 135016.

Fryrear, D.W., 1980. Tillage influences monthly wind erodibility of dryland sandy soils. (pp. 153–163). In Crop Production with Conservation in the 80s. Conference Proceedings, Chicago, IL. 1-2 Dec. American Society of Agricultural Engieneers, (pp. 7–81).

Fryrear, D.W., Saleh, A., Bilbro, J.D., Schromberg, H.M., Stout, J.E. & Zobeck, T.M., 1998. Revised wind erosion equation. USDA Technical Bulletins No 1=

Funk, R., Reuter, H.I., Hoffmann, C., Engel, W. & Öttl, D., 2008. Effect of moisture on fine dust emission from tillage operations on agricultural soils. *Earth Surface Processes and Landforms*, 33, 1851–1863.

Kakavand, S., Mazandarani Zadeh, H. & Ramezani Etedali, H., 2023. Optimal Redistribution of Water among Agricultural Sector Operators Using a Fuzzy Multi-objective Optimization Model. *Irrigation Sciences and Engineering*, 46(1), 77-93.

Kestel, F., Wulf, M. & Funk, R., 2023. Spatiotemporal variability of the potential wind erosion risk in Southern Africa between 2005 and 2019. *Land Degradation & Development*, 34(10), 2945–2960.

Mesbahzadeh, T., Alipour, N., Ahmadi, H., Malekian, A. & Jafari, M., 2018. Time evaluating of dust phenomenon in Alborz and Qazvin provinces. *Journal of environmental studies*, 44(2), 309-320.

Nordstrom, K.F. & Hotta, S., 2004. Wind erosion from cropland in the USA: a review of problems, solutions and prospects. *Geoderma*, 121, 157–167.

Pelous, A. & Taati, A., 2022. Land Use Change Analysis of a Part of Qazvin Plain Using Remote Sensing Techniques. *Proceedings of the 4th National Congress on the Development and Promotion of Agricultural Engineering and Soil Sciences of Iran*.

Rangzan, K. & Balouei, F., 2024. Dust monitoring and investigation of its relationship with topographical, climatic and vegetation factors. *Desert Ecosystem Engineering*, 12(39), 43-60.

Ravi, S., D'Odorico, P., Breshears, D., Field, J., Goudie, A., Huxman, T., Li, L., Okin, G., Swap, R., Thomas, A., Van Pelt, R., Whicker, J. & Zobeck, T.M., 2011. Aeolian process and the biosphere. *Reviews of Geophysics*, 49, 1–45.

Salajegheh, S., Eskandari Damaneh, H. & Eskandari Damaneh, H., 2024. Examining the Spatial and Temporal Relationships among Aerosol Optical Depth, Soil Moisture, and Wind Speed from 2000 to 2024, (Case Study: Western Iran). *Desert*, 29(2), 314-326

Scholes, R.J. & Archer, S.R., 1997. Tree-grass interactions in savannas. *Annual Review of Ecology and Systematics*, 28, 517-544.

Selmy, S.A.H., Abd Al-Aziz, S.H., Jiménez-Ballesta, R., García-Navarro, F.J. & Fadl, M.E., 2021. Modeling and Assessing Potential Soil Erosion Hazards Using USLE and Wind Erosion Models in Integration with GIS Techniques: Dakhla Oasis, Egypt. *Agriculture*, 11, 1124.

Shao, Y., 2008. *Physics and modelling of wind erosion*. Springer: Cologne.

Shobeiri, S. M., Khosravi, H., Azarnivand, H. & Eskandari Damaneh, H., 2024. Spatiotemporal Dynamics of Vegetation Cover and Their Relationships with Climate Change and Land Use in North-Eastern Iran. *Rangeland*, 18(1), 1–22.

Singh, R., 2023. Wind Erosion. In: Soil and Water Conservation Structures Design. *Water Science and Technology Library*, Springer, Singapore, vol 123.

Skidmore, E.L. & Layton, J.B., 1992. Dry-soil aggregate stability as influenced by selected soil properties. *Soil Science Society of America Journal*, 56, 557–561.

Skidmore, E.L., 1986. Wind erosion climatic erosivity. *Climatic Change*, 9, 195–208.

Sterk, G., Herrmann, L. & Bationo, A., 1996. Wind-blown nutrient transport and soil productivity changes in Southwest Niger. *Land Degradation & Development*, 7, 325–335.

TA-Luft., 2001. Erste Allgemeine Verwaltungsvorschrift zum Bundes-Immissionsschutzgesetz. Technische Anleitung zur Reinhaltung der Luft – TA-Luft Stand 12.06.200.

Zahrabi, S., Khosravi, H., Mesbahzadeh, T., Jafari, M. & Dastoorani, M., 2020. Investigation of Wind Erosion Threshold Velocity and Its Dependence on Soil Properties in Dust Source Areas of Alborz Province. *Geographical Studies of Arid Regions*, 10(38), 11–13.

Zandifar, S., Khosroshahi, M. & Ebrahimi Khousfi, Z., 2022. Analysis of the Effect of Drought on Dust Storm Events in Different Regions of Qazvin Province. *Quarterly Journal of Physical Geography*, 15(56), 53–66.

Zhang, Y.M., Wang, H.L., Wang, X.Q., Yang, W.K. & Zhang, D.Y., 2006. The microstructure of microbiotic crust and its influence on wind erosion for a sandy soil surface in the Gurbantunggut Desert of northwestern China. *Geoderma*, 132, 441–449.